Electronic Supplementary Information

Efficiency and active sites of the synergetic sequestration of sorption and photocatalysis in Cr(VI) decontamination on 3D oxidized graphene ribbons framework

Zhe Ding,[abc] Jianjun Liang,[*ab] Wentao Zhang,[abc] Wei Wang,[abc] Rongyue Geng,[abc] Yun Wang,[abc] Ping Li,[ab] and Qiaohui Fan[*ab]

[a] *Northwest Institute of Eco-Environment and Resources, Chinese Academy of Sciences, Lanzhou 730000, China*

[b] *Key Laboratory of Petroleum Resources, Gansu Province, Lanzhou 730000, China*

[c] *University of Chinese Academy of Sciences, Beijing 100049, China*

*Corresponding Authors

E-mail: liangjj@lzb.ac.cn; fanqh@lzb.ac.cn

Total number of Pages: 7

Total number of Tables: 3

Total number of Figures: 3

Materials and instruments

All reagents were not further purified or modified after buy unless mentioned later. PA (the average molecular weight M_w = 15000), multi-wall carbon nanotubes, $K_2Cr_2O_7$ and Cr_2O_3 were purchase from Sigma-Aldrich.

The morphologies of materials were obtained by an Apreo S field emission scanning electron microscope (SEM) and a Tecnai-G2-F30 transmission electron microscope (TEM), respectively. The element compositions and chemical mappings were examined using energy-dispersive spectroscopy (EDS) equipped in TEM. Fourier transform infrared spectroscopy (FT-IR) patterns were measured from 4000 to 400 cm^{-1} with a resolution of 4 cm^{-1} using a Bruker ALPHA spectrometer with pure KBr as the background. X-ray diffraction (XRD) characterization was recorded on an X′ Pert pro Panalytical diffractometer equipped with a rotation anode, operating at 40 kV and 30 mA using Cu Kα radiation. Brunauer-Emmett-Teller (BET) specific surface area and pore parameters were analyzed via the nitrogen isotherms at -196.6 °C in virtue of Micromeritics ASAP 2020. Occurrence states of elements can be perceived with the help of X-ray photoelectron spectroscopy (XPS) measurements using Kratos AXIS Ultra^{DLD} spectrometer with an Al Kα monochromated source. In order to avoid the deviation caused by charge effect, the XPS results were corrected according to C 1s peak at 284.6 eV of the surface adventitious carbon. Cr(VI) concentration and adsorption spectra of the precursors were observed by a Shimadzu UV-2600A spectrophotometer. The valence band (VB) structure was obtained from Thermo Fisher ESCALAB 250Xi with a He I UV source. The photocurrent was conducted on a CHI 660E electrochemical workstation (Shanghai Chenhua, China) using a classical three-electrode system.

Preparation of 3D carbon-based remediation material

We obtained oxidized graphene ribbons (OGRs) via longitudinally unzipping multi-wall carbon nanotubes in concentrated sulphuric acid mixed 600 wt% $KMnO_4$ [1]. After isolation, the OGRs were purified by the dialysis until the remnant manganese ions and sulfate radical cannot be detected by the inductively coupled plasma mass spectroscopy (ICP-MS).

3D carbon framework was prepared according to our previous researches [2,3]. The obtained precursor (OGRs, 50 mg) were dispersed via ultrasonic exfoliation of 30 minutes in 18.2 MΩ·cm H_2O (140 mL) at the 10 °C. Subsequently, 2.5 % dispersion solution of PA crosslinker (8.85 mL) was slowly dropped into homogeneous precursor solutions under ultrasound. The mixture instantly

assembled into the hydrogel. Then, the hydrogel was freeze-dried. The mass ratio of precursor and PA was designed as 1: 2.7. The as-prepared composite was named P-OGR.

Photocurrent tests

The photocurrent response was tested in typical three-electrode system with Pt sheet as counter electrode and Ag/AgCl as reference electrode, respectively [4]. Clear working electrode (FTO glass, active area 1 cm^2) was coated with slurry, composed of 10 mg tested sample, 0.95 mL ethyl alcohol and 50 μL Nafion. The photoelectrochemical cell was filled with 0.1 mol L^{-1} of Na_2SO_4 electrolyte solution. A 300 W Xe lamp was selected as the light source, located 15 cm away from the cell. The transient photocurrent was recorded at intervals of 10 s on-off cycles.

Photo-sequestration kinetics of Cr(VI)

OGRs or P-OGR suspension, deionized water, NaCl and Cr(VI) stock solutions were accurately weighed and added into the quartz beaker to gain the target concentrations (the mass-to-volume (m/V) = 0.2 g L^{-1} for OGRs, and 0.5 g L^{-1} for P-OGR, I = 0.5 mM NaCl, and $C_{initial\ Cr(VI)}$ = 2.0 mM). The total volume of the dispersion was set as 500 mL, and pH value was adjusted to be 5.70. Firstly, the beaker stood in the dark for 1 h to ensure the sorption equilibrium. Next, a 300 W Xe lamp was turned on for the stable irradiation, located 15 cm away from the test beaker (in P-OGR experiments, both sunlight and Xe lamp were used). The samples were periodically collected and filtrated with 0.22 μm filter membranes. Then, the solids were freeze-dried in the dark, accurately weight, and performed FT-IR analysis to evaluate Cr occurrence states. Cr(VI) concentrations in the filtrates were determined via the colorimetric method.

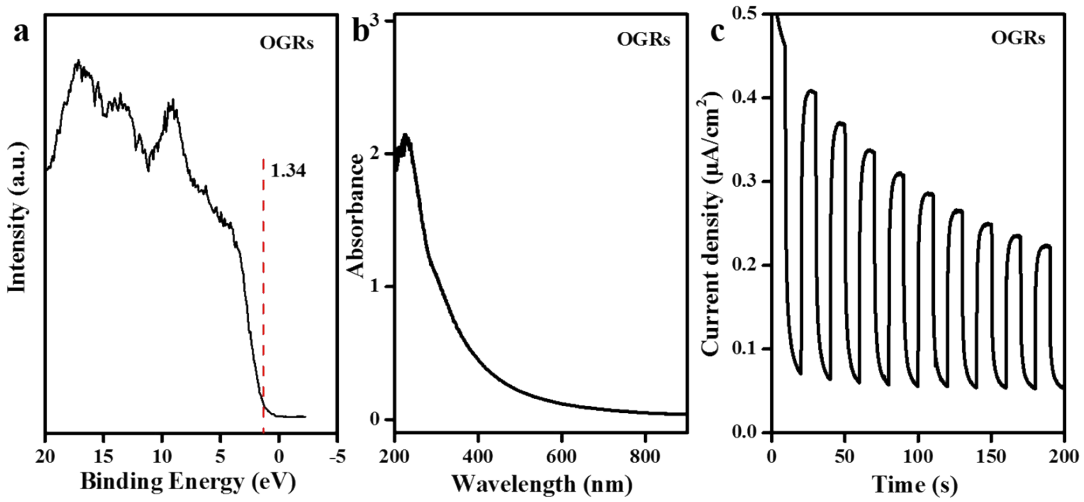

Fig. S1. (a) The valence band structure, (b) UV-vis absorbance spectra and (c) transient photocurrent response of OGRs.

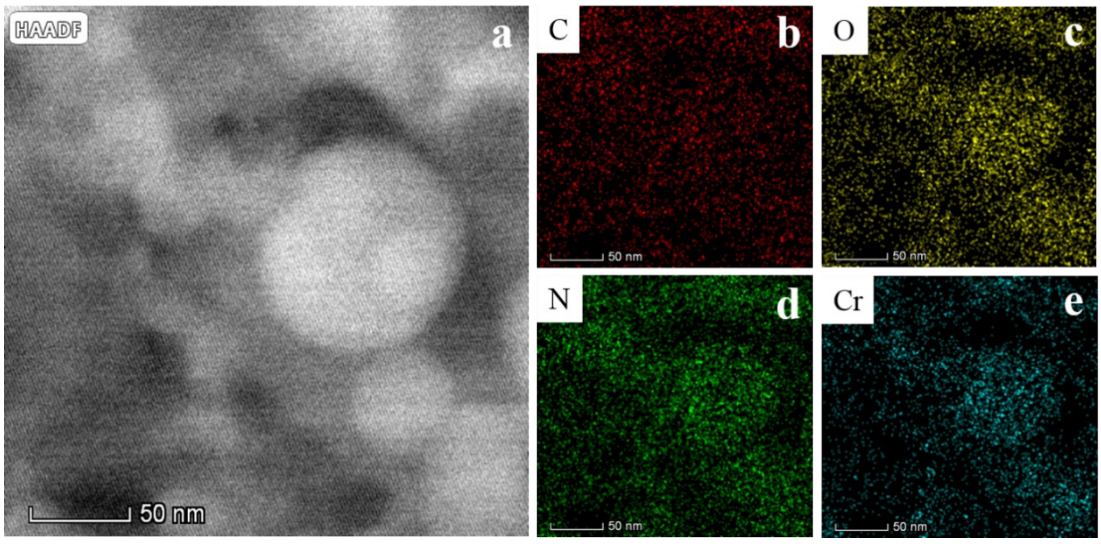

Fig. S2. Mapping profiles of P-OGR with the loading of Cr: (a) the scanning scope, and the element distributions of (b) carbon, (c) oxygen, (d) nitrogen, (e) chromium (T = 298 ± 1 K, I = 0.5 mM NaCl, $C_{initial\ Cr(VI)}$ = 5.8 mM and the mass to volume (*m/V*) = 0.5 g L^{-1})

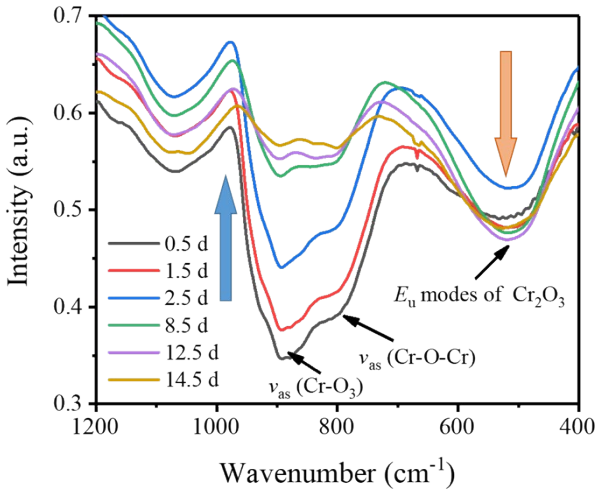

Fig. S3. FT-IR spectra of Cr(VI) photo-sequestration procedure on P-OGR (I = 0.5 mM NaCl, pH = 5.7, *m/V* = 0.5 g/L). notes: the tests were conducted in spring, all others were done in autumn. Because of lower temperature and shorter sunlight times in spring, Cr(VI) photoreduction was prolonged to 14.5 days.

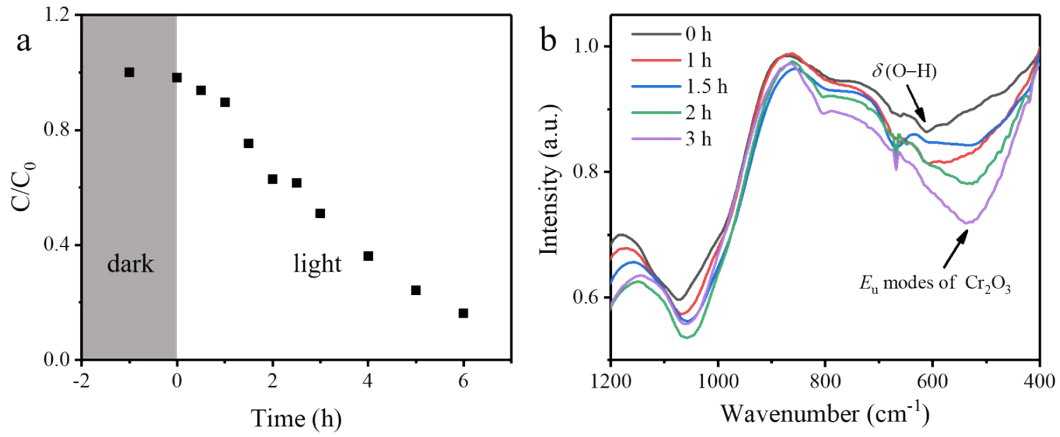

Fig. S4. (a) Photo-sequestration kinetics of Cr(VI) on OGRs under the illumination of 300 W Xe lamp, (b) FT-IR analyses of Cr(VI) photo-sequestration on OGRs (I = 0.5 mM NaCl, pH = 5.7, $C_{initial\ Cr(VI)}$ = 2.0 mM, *m/V* = 0.2 g/L).

In the dark, electrostatic repulsion between OGRs and Cr(VI) anions resulted in a negligible sorption capacity for Cr(VI). As the irradiation started, Cr(VI) concentration showed an obvious decline, and ~ 84 % Cr(VI) were removed after 6 hours (as shown in Fig. S4a). FT-IR suggested the absence of Cr(VI) characteristic bands at 890 cm^{-1} and 800 cm^{-1}, indicating that scarce Cr(VI) was adsorbed on the surface of OGRs (Fig. S4b). Along with the irradiation of Xe lamp, E_u modes of Cr_2O_3 turned obvious at 530 cm^{-1}, suggesting that Cr(VI) was photo-sequestrated and transformed into Cr_2O_3 on OGRs.

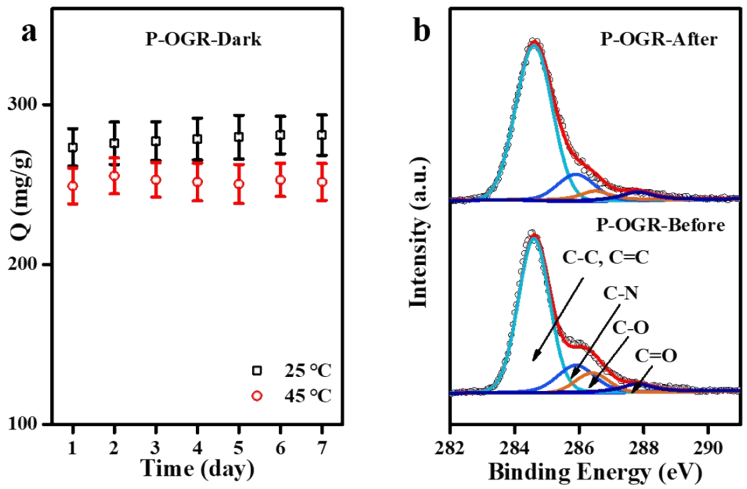

Fig. S5. (a) Photothermic effect on Cr(VI) decontamination, (b) C1s fine spectra in P-OGR before and after the reaction in the dark (T = 298 ± 1 K, I = 0.5 mM NaCl, $C_{initial\ Cr(VI)}$ = 5.8 mM and *m/V* = 0.5 g L^{-1}).

Table S1 The C1s fine spectra of P-OGR.

Sample	C-C, C=C		C-N		C-O		C=O	
	Binding Energy (eV)	Relative Area	Binding Energy (eV)	Relative Area	Binding Energy (eV)	Relative Area	Binding Energy (eV)	Relative Area
OGRs	284.6	47.19%	—	—	286.75	38.97%	288.39	13.85%
P-OGR	284.60	69.31%	285.90	16.08%	286.40	8.97%	287.80	5.64%

Table S2 The BET profiles of P-OGR.

Materials	BET surface area ($m^2\ g^{-1}$)	Total pore volume ($\times 10^{-3}\ cm^3\ g^{-1}$)	Average pore width (nm)
P-OGR	2.05	3.04	4.79

Table S3 The comparison of C1s XPS results on the P-OGR before and after reacting with Cr(VI).

Sample	C-C, C=C		C-N		C-O		C=O	
	Binding Energy (eV)	Relative Area	Binding Energy (eV)	Relative Area	Binding Energy (eV)	Relative Area	Binding Energy (eV)	Relative Area
P-OGR-Before	284.60	69.31%	285.90	16.08%	286.40	8.97%	287.80	5.64%
P-OGR-After	284.60	74.31%	285.90	13.68%	286.50	6.43%	287.80	5.58%

■ REFERENCES

1 D.V Kosynkin, A.L. Higginbotham, A. Sinitskii, J.R. Lomeda, A. Dimiev, B.K. Price and J.M. Tour, *Nature*, 2009, **458**, 872–876.

2 J. Liang, B. He, P. Li, J. Yu, X. Zhao, H. Wu, J. Li, Y. Sun and Q. Fan, *Chem. Eng. J.*, 2019, **358**, 552–563.

3 J. Liang, Z. Ding, H. Qin, J. Li, W. Wang, D. Luo, R. Geng, P. Li and Q. Fan, *Environ. Pollut.*, 2019, **251**, 945–951.

4 J. Zhang, J. Yu, M. Jaroniec and J. R. Gong, Nano Lett. 2012, **12**, 4584–4589.